Available online at www.sciencedirect.com
ScienceDirect
Journal of Sound and Vibration 300 (2007) 466–478
JOURNAL OF SOUND AND VIBRATION
www.elsevier.com/locate/jsvi

A study on annular plates with radial through cracks by means of sector type element

A. Demir, Vahit Mermertaş*

Faculty of Mechanical Engineering, Technical University of Istanbul, 34439 Gümüşsuyu-İstanbul, Turkey

Received 31 August 2004; received in revised form 28 June 2005; accepted 1 March 2006
Available online 7 November 2006

Abstract

In this study, the natural frequencies of annular plates with periodic radial through cracks are investigated by means of finite element method. The position of the crack in the plate surface was selected as parallel to radial direction. Both the cracks emanating from the inner and outer boundary of the plate is non-propagating and open. The crack in the element was modeled by an additional flexibility matrix, the terms of which were calculated using fracture mechanics. For this purpose, an isoparametric sector type element with radial through crack of four nodes and three degrees of freedom at each node is considered. In the event of the selection of appropriate half sector angle, taking into account the closeness of the geometries of the sector and trapezoidal type element, the flexibility matrix of the sector type element with crack are derived by means of the flexibility matrix of the trapezoidal type element. The natural frequencies of annular plates are found for different length and number of cracks. The theoretical results are obtained with different boundary conditions. The obtained results of improved elements are compared with experimental results in the literature. It is observed that the increment of the length and number of cracks has various effects on the natural frequencies and mode shapes of the annular plate.

1. Introduction

The existence of a crack on a plate increases the local flexibility of the plate. The influence of cracks on dynamic characteristics such as changes in natural frequencies, modes of vibration of structures has been the subject of many investigations. A comprehensive survey of the literature concerning the vibrations of cracked structures has recently made by Dimarogonas. The different modeling techniques for cracked structures are given in Ref. [1]. The vibrations of a cracked rectangular plate were investigated by Stahl and Keer [2]. Solecki [3] examined the problem of the bending vibrations of a simply supported rectangular plate with a crack parallel to one edge by means of finite Fourier transformation of discontinuous functions. Qian et al. [4] studied the finite element model of cracked plates. They derived the element stiffness matrix of the plate from integration of stress intensity factors. Lee and Lim [5] presented a numerical method based on the Rayleigh method for predicting the natural frequencies of a rectangular plate with a centrally located crack including

*Corresponding author. Fax: +90 212 2450795.
E-mail address: mermertas@itu.edu.tr (V. Mermertaş).

0022-460X/$ - see front matter © 2006 Elsevier Ltd. All rights reserved.
doi:10.1016/j.jsv.2006.03.057

transverse shear deformation and rotary inertia. Krawczuk [6] examined the effects of the crack location and its length on the changes of the natural frequencies of the simply supported and cantilever rectangular plate. Liew et al. [7] investigated the vibration behavior of cracked rectangular plates. They analyzed the vibrations of rectangular plates with a crack emanating from an edge or centrally located. Khadem and Rezaee [8] presented an analytical approach to the crack detection of rectangular plates under uniform external loads using vibration analysis. Krawczuk et al. [9] studied the finite element model of plate with elasto-plastic through crack. They used the element based on elasto-plastic fracture mechanics and the finite element method.

Unfortunately, only a few papers have been published so far on the vibration analysis of cracked annular plates. Lee [10] proposed a simple numerical method based on Rayleigh principle for predicting the fundamental frequencies of an annular plate with an internal concentric crack. He applied the method for annular plates with two edges simply supported and two edges clamped. Ramesh et al. [11] reported an experimental investigation on the effects of the number and length of periodic radial cracks on the natural frequencies of an annular plate. Anifantis et al. [12] analyzed the vibration of cracked annular plates. They modeled a surface peripheral crack of an annular plate as a local rotational flexibility for vibration analysis. Yuan et al. [13] presented a Ritz solution for the determination of the natural frequencies of free vibration of circular and annular plates with radial or circumferential cracks or slits through the full thickness. They used the minimum number of sector plate elements, which are joined together by means of artificial springs.

The purpose of this study is to obtain the flexibility matrix of the sector type element with radial through crack by using the formulas of the trapezoidal type element in case of setting close geometric dimensions, and to prove the applicability of this derived element in the dynamic analysis of annular plates with cracks. When the results attained are compared to the experimental results in the literature, the same outcome is found and its interpretations are presented.

2. The trapezoidal type element with through crack

The geometry of the trapezoidal type element with through crack is shown in Fig. 1. It has four nodes, 12 degrees of freedom (dof) and the thickness is uniform along the whole body. The dof per node are the displacement in the z direction and the rotations around the x and y axes of lines originally normal to the middle plane of the plate before deformation.

The nodes of the element are subjected to nodal forces (S_1–S_{12}) as shown in Fig. 2a. These nodal forces are linearly dependent. Using equations for the overall equilibrium, these forces can be expressed by a system of nine independent nodal forces [14].

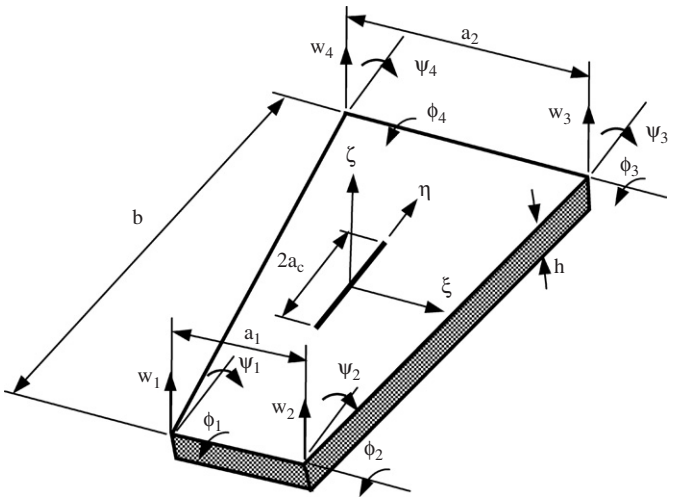

Fig. 1. The trapezoidal type element with a through crack.

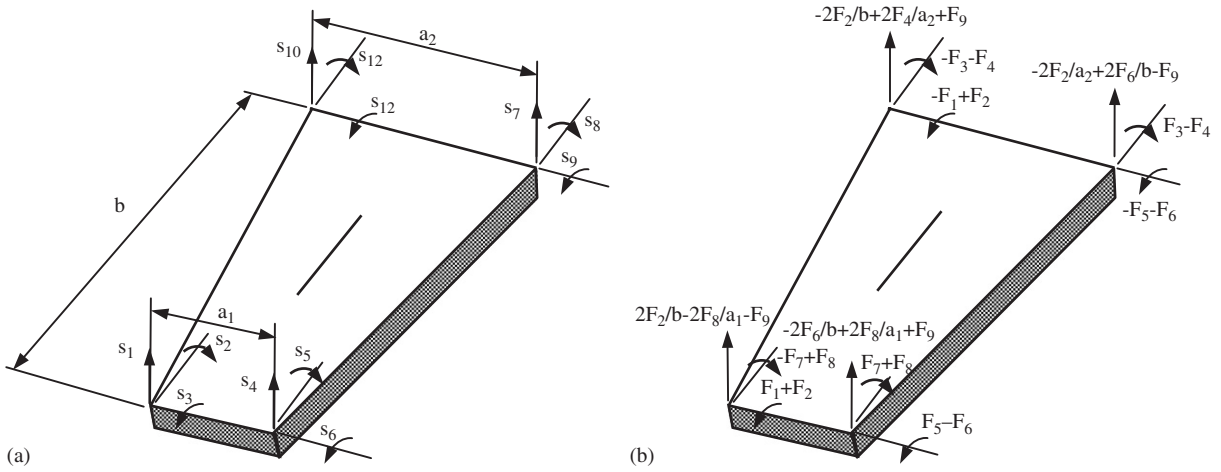

Fig. 2. Nodal forces of the trapezoidal type element with the through crack: (a) the system of dependent nodal forces (S_1–S_{12}) and (b) the system of independent nodal forces (F_1–F_9).

As shown in Fig. 1, the position of the crack in the plate surface was selected as parallel to η direction. The stiffness matrix $\mathbf{k}_{tc}$ of the analyzed element with crack can be written in the following form [6]:

$$\mathbf{k}_{tc} = \mathbf{T}(\mathbf{C}_t^0 + \mathbf{C}^1)^{-1}\mathbf{T}^{\mathrm{T}}, \tag{1}$$

where $\mathbf{C}_t{}^0$ is the flexibility matrix of the non-cracked element, $\mathbf{C}^1$ is the flexibility matrix due to the presence of the crack. Assuming that the normal stresses vary linearly and the shearing stresses are constant, the flexibility matrix $\mathbf{C}_t{}^0$ can be obtained [4].

Nodal forces at 2, 3 and 4 are selected as independent ones

$$\begin{Bmatrix} \mathbf{S}_r \\ \mathbf{S}_f \end{Bmatrix} = \begin{bmatrix} \mathbf{k}_{t11} & \mathbf{k}_{t12} \\ \mathbf{k}_{t21} & \mathbf{k}_{t22} \end{bmatrix} \begin{Bmatrix} \boldsymbol{\delta}_r \\ \boldsymbol{\delta}_f \end{Bmatrix}, \tag{2}$$

$$\begin{aligned} \mathbf{S}_r &= \{ S_1 \quad S_2 \quad S_3 \}^{\mathrm{T}}, \\ \mathbf{S}_f &= \{ S_4 \quad S_5 \quad \cdots \quad S_{12} \}^{\mathrm{T}}, \\ \boldsymbol{\delta}_r &= \{ \delta_1 \quad \delta_2 \quad \delta_3 \}^{\mathrm{T}}, \\ \boldsymbol{\delta}_f &= \{ \delta_4 \quad \delta_5 \quad \cdots \quad \delta_{12} \}^{\mathrm{T}}. \end{aligned} \tag{3}$$

In order to calculate flexibility matrix of the trapezoidal element, node 1 is constrained, i.e.

$$\boldsymbol{\delta}_r = \mathbf{0}.$$

From Eq. (2),

$$\boldsymbol{\delta}_f = \mathbf{k}_{t22}^{-1}\mathbf{S}_f, \tag{4}$$

$$\mathbf{S}_r = \mathbf{k}_{t12}\mathbf{k}_{t22}^{-1}\mathbf{S}_f. \tag{5}$$

Under a selected independent system, the flexibility matrix is

$$\mathbf{C}_t^0 = \mathbf{k}_{t22}^{-1}. \tag{6}$$

The equilibrium condition of the element is

$$\begin{Bmatrix} \mathbf{S}_r \\ \mathbf{S}_f \end{Bmatrix} = [\mathbf{T}]_{12\times 9}\{\mathbf{S}_f\}, \tag{7}$$

where the transformation matrix $\mathbf{T}$ is

$$\mathbf{T} = \left[\frac{\mathbf{k}_{t12}\mathbf{k}_{t22}^{-1}}{\mathbf{I}_{9\times 9}} \right]_{12\times 9}. \tag{8}$$

By means of equations for the overall equilibrium, the matrix $\mathbf{T}$ transforms the nodal forces (S_1–S_{12}) to the independent nodal forces as shown in Fig. 2b ($F_i = S_{i+3}$, $i = 1, 9$).

Due to the crack occurring in the element, the flexibility matrix $\mathbf{C^1}$ of the element consists of the terms which can be calculated by using the following relationship [14]

$$c_{ij}^1 = \frac{\partial^2 U^1}{\partial F_i \, \partial F_j} \quad (i = 1, 9;\ j = 1, 9). \tag{9}$$

In this equation, F_i, F_j are the independent nodal forces acting on the element, U^1 is the energy of strain deformation of the element due to the crack.

For the plane stresses, the energy of strain deformation of the element due to the crack, can be written in the following form

$$U^1 = \frac{1}{E} \int_A \left(\sum_{i=1}^{i=9} K_{Ii}^2 + \sum_{i=1}^{i=9} K_{IIi}^2 \right) \mathrm{d}A, \tag{10}$$

where K_{ji} ($j = I, II$; $i = 1, 9$) are the stress intensity factors corresponding to two models of crack evaluation (j), and to independent nodal forces (i), A is the area of the crack. The normal and the shear stresses acting on the surface of crack for rectangular plate element are given in Ref. [6]. When a stress analysis is performed for the trapezoidal type element, the normal and the shear stresses acting along the radial crack which is located in the middle of the finite element are the same with those of the rectangular element. Therefore, stresses given in Ref. [6] are also valid for the trapezoidal element.

After a series of calculations, finally, the matrix $\mathbf{C}^1$ can be obtained as follows [6]:

$$\mathbf{C}^1 = \frac{6\pi}{Eh^3} \begin{bmatrix} 0 & & & & & & & & \\ 0 & 0 & & & & & & & \\ 0 & 0 & c_{33} & & & & & & \\ 0 & 0 & 0 & 0 & & & \text{symmetric} & & \\ 0 & 0 & 0 & 0 & 0 & & & & \\ 0 & 0 & 0 & 0 & 0 & 0 & & & \\ 0 & 0 & c_{73} & 0 & 0 & 0 & c_{77} & & \\ 0 & 0 & 0 & 0 & 0 & 0 & 0 & 0 & \\ 0 & 0 & 0 & 0 & 0 & 0 & 0 & 0 & c_{99} \end{bmatrix} \tag{11}$$

where h is the thickness of the element, the nonzero terms of the matrix $\mathbf{C}^1$ have the forms

$$c_{33} = 4\kappa_1^2 \int_{-g_k}^{g_k} g(0.5 + 0.75g)^2 f_c^2(g)\, \mathrm{d}g, \tag{12a}$$

$$c_{73} = 2\kappa_1^2 \int_{-g_k}^{g_k} g(0.5 + 0.75g)(0.5 - 0.75g) f_c^2(g)\, \mathrm{d}g, \tag{12b}$$

$$c_{77} = 4\kappa_1^2 \int_{-g_k}^{g_k} g(0.5 - 0.75g)^2 f_c^2(g)\, \mathrm{d}g, \tag{12c}$$

$$c_{99} = b^2\kappa_2^2 \int_{-g_k}^{g_k} g f_c^2(g)\, \mathrm{d}g, \tag{12d}$$

where $g_k = 2a_c/b$, κ_1 and κ_2 are the correction functions given in Ref. [6] and

$$f_c(g) = 1 + 0.01876g + 0.1825g^2 + 2.024g^3 - 2.4316g^4. \tag{13}$$

Using the relationship between Eqs. (1), (6), (8) and (11), the stiffness matrix $\mathbf{k}_{tc}$ of the trapezoidal element with crack can be calculated. Since the crack is assumed to change only the stiffness of the element, mass matrix of the element has the same form as the mass matrix of the non-cracked element [14].

3. The sector type element with through crack

The geometric configuration of the sector type element with through crack is shown in Fig. 3. The sector type element has four nodes, 12 dof. r_1 and r_2 are inner and outer radius of the sector type element, respectively. α is the half sector angle.

Using the closeness of the geometries, the stiffness matrix of the sector type element with a radial through crack located centrally is obtained by means of the stiffness matrix of the trapezoidal type element with a through crack located centrally. The dimensions of the trapezoidal type element shown in Fig. 1 can be expressed in the following form by means of the sector element's dimensions α, r_1 and r_2.

$$\begin{aligned} a_1 &\cong 2r_1 \sin\alpha, \\ a_2 &\cong 2r_2 \sin\alpha, \\ b &= (r_2 - r_1)\cos\alpha. \end{aligned} \tag{14}$$

In this case, a sector type element which has the same straight edges completely and the other two edges with a little error are taken up. For the values of the angle α in terms of radian, this relative error can be written

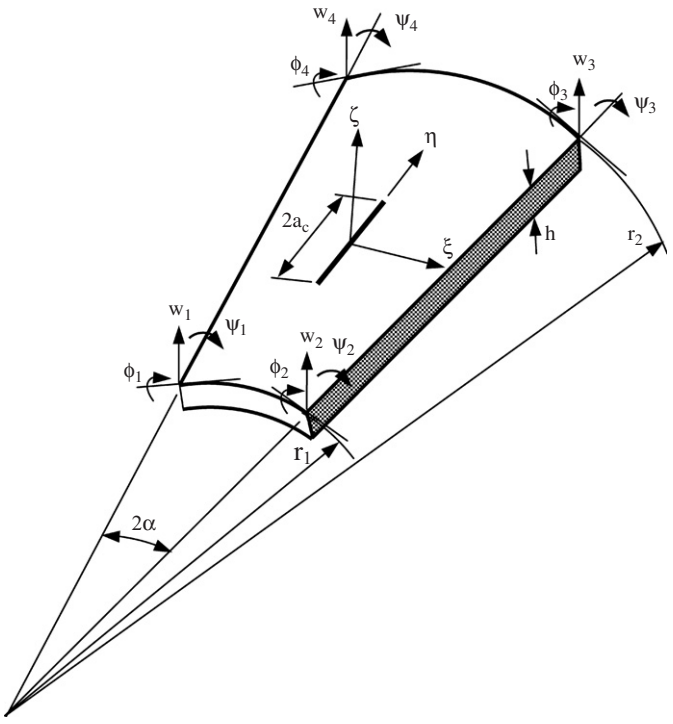

Fig. 3. The sector type element with a radial through crack.

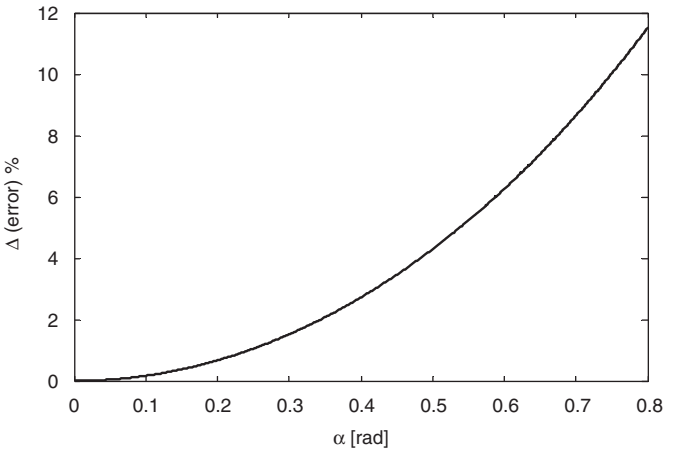

Fig. 4. The graph of dimension error of sector element with respect to the trapezoidal element (Δ(error)).

with respect to the trapezoidal type element in the following form:

$$\Delta(\text{error})\% = \frac{\alpha - \sin\alpha}{\sin\alpha} 100. \tag{15}$$

In Fig. 4, the values of the dimension error are given with respect to changes in the half sector angle. As the half sector angle α expands, dimension error Δ also moves upward while geometric closeness between the trapezoidal type and sector type elements disappears for the higher values of the angle α. In this study, $\alpha = 0.06545$ rad is used for the half sector angle of sector type element, then the dimension error is $\Delta(\text{error}) = 0.07\%$.

The displacements ($\mathbf{q}_{\text{sector}}$) of the sector type element shown in Fig. 3 are transformed into the Cartesian coordinates ($\mathbf{q}_{\text{trapezoidal}}$) used in nodal points of the trapezoidal type element shown in Fig. 1 by using the matrix $\mathbf{L}_r$ which is given below.

$$\mathbf{q}_{\text{sector}} = \mathbf{L}_r \mathbf{q}_{\text{trapezoidal}}, \tag{16}$$

$$\mathbf{L}_r = \begin{bmatrix} \mathbf{L_1} & \mathbf{0} & \mathbf{0} & \mathbf{0} \\ \mathbf{0} & \mathbf{L_2} & \mathbf{0} & \mathbf{0} \\ \mathbf{0} & \mathbf{0} & \mathbf{L_2} & \mathbf{0} \\ \mathbf{0} & \mathbf{0} & \mathbf{0} & \mathbf{L_1} \end{bmatrix}, \quad \mathbf{L}_1 = \begin{bmatrix} 1 & 0 & 0 \\ 0 & -\sin\alpha & -\cos\alpha \\ 0 & \cos\alpha & -\sin\alpha \end{bmatrix}, \quad \mathbf{L}_2 = \begin{bmatrix} 1 & 0 & 0 \\ 0 & \sin\alpha & -\cos\alpha \\ 0 & \cos\alpha & \sin\alpha \end{bmatrix}, \tag{17}$$

When the elements of the stiffness matrix, which is obtained in terms of the Cartesian coordinates of the non-cracked sector element and the dimensions adopted in this study are compared with those of the stiffness matrix of the non-cracked trapezoidal element expressed in terms of the same coordinates, average error is realized around 0.45%.

After the operation of transforming into the Cartesian coordinates is completed, the flexibility matrix $\mathbf{C}_s^0$ of the non-cracked element is obtained by means of Eq. (6). By adding the matrix $\mathbf{C}^1$ given with Eq. (11) to the flexibility matrix $\mathbf{C}_s^0$ representing the non-cracked element, the flexibility matrix of the element with crack is established. Applying the similar expression shown in Eq. (1) to the element, the stiffness matrix of the element with crack is obtained for the Cartesian coordinates. Later, the obtained stiffness matrix is transformed into the original coordinates of the sector type element.

The mass matrix of the element with through crack has the same form as the mass matrix of the non-cracked element.

Neglecting damping and preloads, natural frequencies of the analyzed system are defined by the well-known equation,

$$\mathbf{K} - \omega_{ij}^2 \mathbf{M} = \mathbf{0}, \tag{18}$$

where $\mathbf{M}$ is the global matrix of mass, $\mathbf{K}$ the global matrix of stiffness, i the number of nodal diameters, j the number of nodal circles and ω_{ij} the natural frequencies of the annular plate.

4. Numerical results

The finite element model of the annular plate is formed by dividing the plate into 20×48 elements along the radial and angular directions as shown in Fig. 5, respectively. The used plate is the same with the used plate for

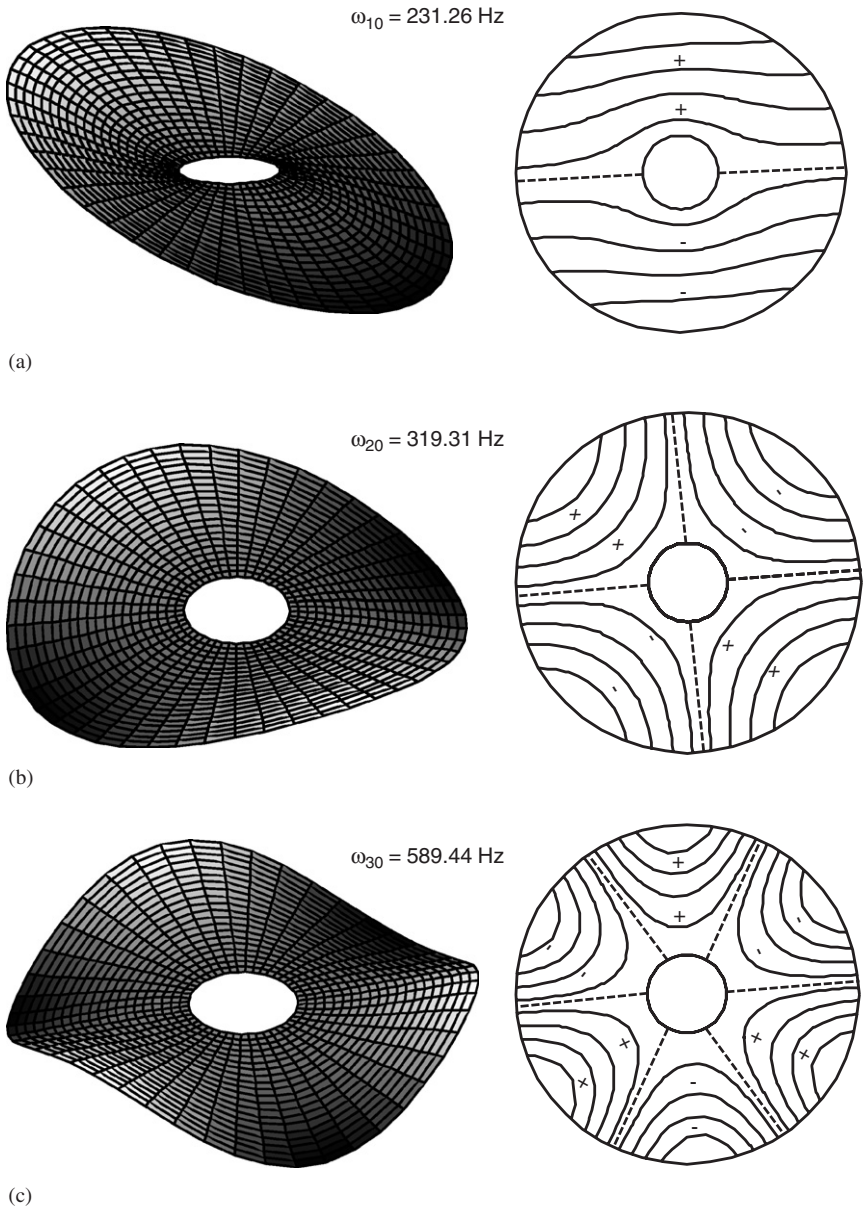

Fig. 5. The first three diametral mode shapes of the non-cracked C–F annular plate: (a) first diametral mode (1,0), (b) second diametral mode (2,0) and (c) third diametral mode (3,0) (- - - - -: nodal points).

experimental study in Ref. [11] to verify the theoretical model. The inner diameter of the plate 60 mm, the outer diameter is 260 mm. The material of the plate is aluminum sheet of 3.18 mm thickness. The properties of the aluminum plate are $\rho = 2720\,\mathrm{kg/m^3}$, $E = 6.9 \times 10^9\,\mathrm{N/m^2}$, $\upsilon = 0.33$.

Annular plates with periodic radial through cracks emanating from both the inner and outer boundary are investigated for various boundary conditions, number of cracks and various crack lengths. The theoretical results are carried out with 4, 6, 12 cracks, 40, 75 mm crack lengths and F–C (free inside and clamped outside case), C–F (clamped inside and free outside case), C–C (clamped inside and clamped outside case), S–S (simply-supported inside and simply-supported outside case) boundary conditions.

Using finite element method, the vibration mode shapes of the analyzed annular plate are theoretically obtained with the eigenvector analysis. Fig. 5 shows natural frequencies and the first three diametral mode shapes of non-cracked annular plate.

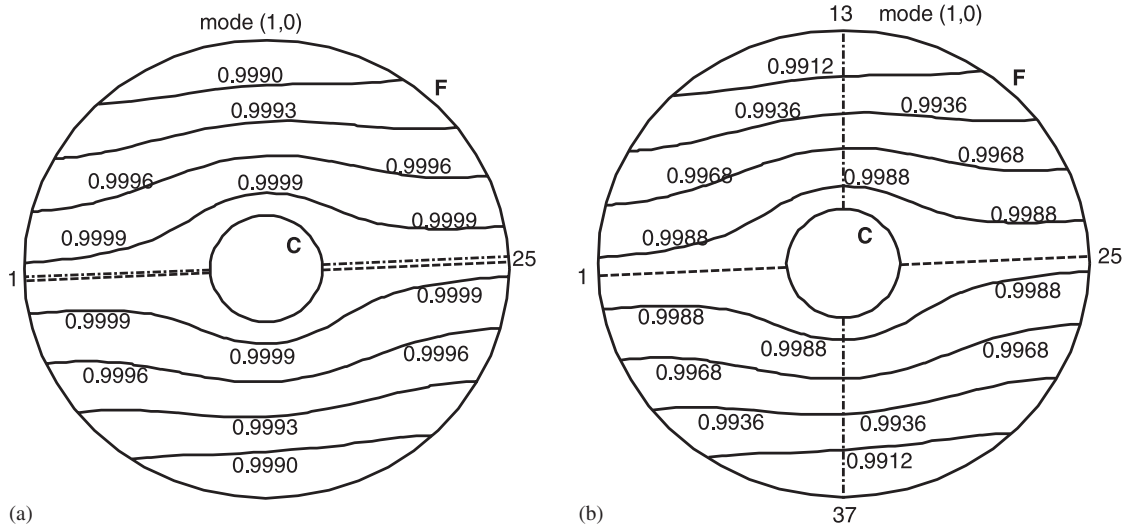

Fig. 6. Relative changes in the first diametral mode shape of the cracked C–F annular plate: (a) cracks located nearest by nodal points, (b) cracks located distant from nodal points (- - - - -: nodal points , - · - · - · : locations of cracks).

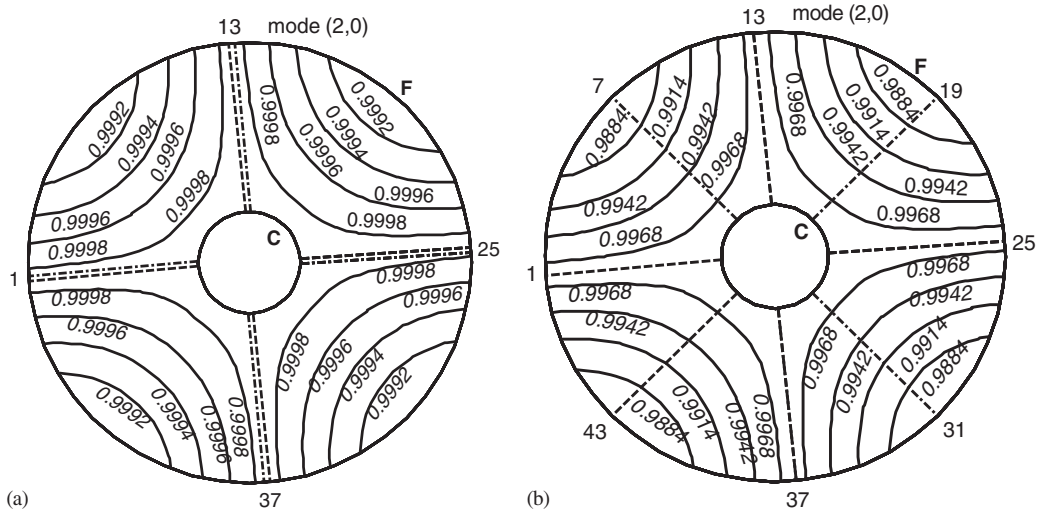

Fig. 7. Relative changes in the second diametral mode shape of cracked C–F annular plate: (a) Cracks located nearest by nodal points and (b) cracks located distant from nodal points (- - - - -: nodal points, - · - · - · : locations of cracks).

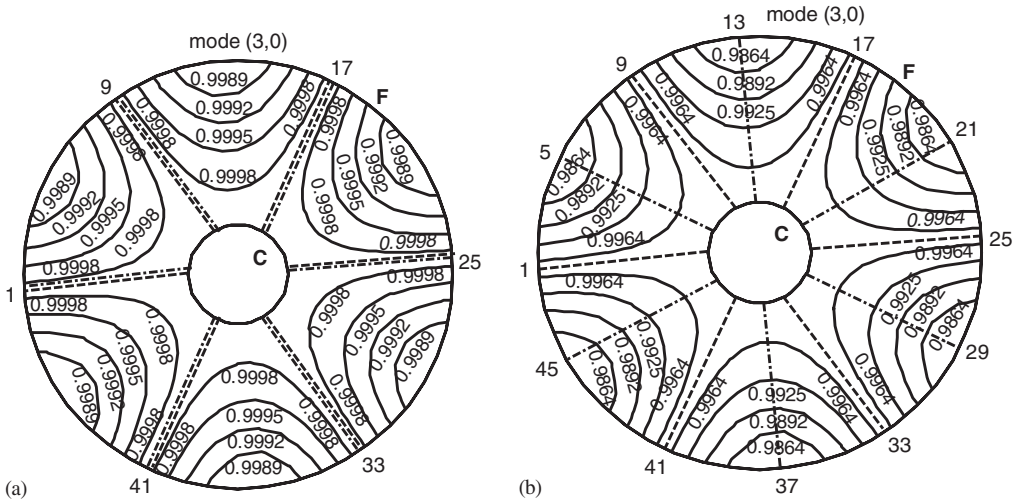

Fig. 8. Relative changes in the third diametral mode shape of cracked C–F annular plate: (a) cracks located nearest by nodal points, and (b) cracks located distant from nodal points (-----: nodal points, - - - - - -: locations of cracks).

Table 1
The natural frequencies ω_{ij} (Hz) and modes (i,j) for C–F annular plate with radial cracks with respect to the locations of cracked element in angular direction ($r_{in} = 60$ mm, $r_{out} = 260$ mm, $h = 3.18$ mm)

Boundary condition	Number of cracks	Locations of cracked elements in angular direction (the numbers of sector group)	ω_{ij} and (i,j)
C–F		No crack	231.26 (1,0)
	2	1[a], 25[a]	230.96 (1,0)
	2	13, 37	228.14 (1,0)
		No crack	319.31 (2,0)
	4	1[a], 13[a], 25[a], 37[a]	318.89 (2,0)
	4	7, 19, 31, 43	315.24 (2,0)
		No crack	589.44 (3,0)
	6	1[a], 9[a], 17[a], 25[a], 33[a], 41[a]	588.49 (3,0)
	6	5, 13, 21, 29, 37, 45	583.71 (3,0)

[a]Positions located nearest nodal diameter belonging to concerned modes.

The influence of the locations of crack on the relative changes of the mode shapes is examined. The achieved results are shown in Figs. 6–8.

Table 1 shows the natural frequencies of the first three diametral mode shapes for C–F annular plate with radial cracks with respect to the locations of cracked elements in angular direction. As it can be shown that, radial through cracks have a reducing effect on the natural frequencies, the cracks are located toward the outer edge from the inner edge of the plate and lengths of the cracks are 100 mm. The cracks in the plate are located into the sector groups in radial directions of the plate. There are 48 sector groups in the plate and each sector group consists of 20 sector element. Figs. 6–8 display the locations of cracks and relative changes of the first three diametral mode shapes of cracked annular plate as contour graphs. As the eigenvalues in Table 1 are studied together with Figs. 6–8, the influence of the cracks on the eigenvalues are explained.

As it can be observed in Table 1, if the two radial cracks are located on the 1st and 25th sector groups which are the closest situations to the nodal diameters of the mode shape (1,0), the decline in the natural frequencies is at its lowest level. In this case relative changes on the mode shape contours is also at its lowest as can be seen in Fig. 6a. In the case that the same two cracks are positioned on the 13th and 37th sector groups farthest from

Table 2
The natural frequencies ω_{ij} (Hz) of the plate with periodic radial through crack emanating from inner boundary for the different boundary conditions

Modes (i,j)	Number of cracks	F-C The length of cracks		C-F The length of cracks		C-C The length of cracks		S-S The length of cracks	
		40 mm	75 mm	40 mm	75 mm	40 mm	75 mm	40 mm	75 mm
(0,0)	4	481.72	480.21	233.22 (241)*	229.35 (225)*	1720.31	1718.52	830.43	828.58
	6	478.86	477.42	231.25 (234)*	220.11 (203)*	1717.92	1715.13	828.66	827.33
	12	476.49	475.48	206.19 (220)*	204.34 (190)*	1716.23	1714.54	827.49	825.95
(1,0)	4	882.45	881.18	203.35 (198)*	202.33 (195)*	1748.43	1746.95	928.61	927.46
	6	881.61	879.64	204.72 (205)*	201.16 (188)*	1746.13	1745.11	926.52	924.55
	12	879.75	876.43	202.91 (200)*	200.65 (180)*	1744.44	1742.82	924.32	921.34
(2,0)	4	1452.27	1450.88	312.17 (294)*	309.49 (292)*	2031.52	2030.35	1262.18	1259.83
	6	1451.94	1452.36	310.76 (293)*	311.27 (300)*	2032.41	2031.42	1260.47	1260.19
	12	1449.79	1449.44	311.12 (299)*	309.54 (281)*	2030.21	2030.67	1258.32	1258.03
(3,0)	4	2552.51	2551.11	579.87 (583)*	572.23 (567)*	2512.44	2511.02	1704.75	1702.46
	6	2550.12	2552.38	577.96 (582)*	574.02 (580)*	2510.15	2509.07	1706.55	1703.24
	12	2549.64	2549.13	575.84 (578)*	567.32 (525)*	2508.54	2510.21	1702.11	1697.18
(4,0)	4	7563.89	7558.95	1743.96	1737.18	4758.31	4758.72	4552.22	4550.55
	6	7567.29	7560.12	1740.29	1739.72	4756.29	4759.13	4553.38	4551.68
	12	7561.15	7555.62	1738.82	1734.66	4552.39	4752.13	4550.32	4547.94
(5,0)	4	3403.13	3401.73	2259.54	2252.08	6642.71	6638.08	5215.35	5211.27
	6	3405.57	3403.22	2256.24	2254.12	6640.46	6639.62	5212.43	5209.34
	12	3401.71	3399.11	2254.23	2249.99	6639.72	6635.36	5210.55	5208.26
(6,0)	4	6762.28	6758.04	2655.17	2649.93	9312.77	9308.46	5398.57	5395.23
	6	6758.21	6759.83	2652.46	2651.02	9309.42	9309.04	5400.46	5396.32
	12	6754.52	6753.12	2649.75	2644.66	9307.33	9304.93	5395.14	5391.93
(0,1)	4	2092.35	2090.12	1609.33 (1549)*	1606.41 (1525)*	5619.26	5616.75	3143.37	3141.25
	6	2090.22	2087.59	1606.24 (1544)*	1603.34 (1506)*	5615.49	5612.53	3140.31	3136.18
	12	2085.22	2082.66	1601.55 (1529)*	1598.25 (1456)*	5610.21	5606.96	3133.84	3126.64
(0,2)	4	4120.24	4117.12	7618.28	7613.52	12343.2	12338.46	7012.72	7005.58
	6	4117.69	4115.08	7613.41	7610.82	12328.1	12331.01	7003.51	7000.67
	12	4112.73	4109.16	7607.44	7605.31	12315.8	12319.78	6996.23	6992.52
(1,1)	4	2193.74	2190.82	1804.19	1802.43	5743.51	5741.73	3349.85	3346.66
	6	2188.13	2186.26	1802.32	1799.29	5740.81	5738.89	3345.56	3342.26
	12	2185.22	2183.65	1799.36	1797.53	5736.11	5733.42	3343.35	3338.34
(2,1)	4	2667.84	2663.25	2057.91	2052.23	7121.22	7119.63	3758.13	3752.99
	6	2664.73	2661.15	2054.04	2048.02	7119.54	7116.08	3755.54	3748.25
	12	2662.12	2658.14	2045.38	2042.02	7111.13	7111.07	3750.62	3742.73
(3,1)	4	4300.26	4298.26	2542.33	2538.23	7568.23	7563.38	4459.34	4456.19
	6	4296.55	4293.42	2538.47	2435.16	7562.24	7560.85	4456.73	4452.45
	12	4292.22	4290.35	2504.76	2494.79	7558.19	7556.55	4452.31	4449.32
(4,1)	4	3361.11	3360.88	3463.22	3461.41	8452.77	8449.93	7917.15	7912.81
	6	3358.29	3356.12	3460.44	3458.26	8445.53	8443.47	7913.62	7910.34
	12	3356.22	3353.35	3458.24	3455.62	8441.48	8437.81	7910.32	7907.12
(1,2)	4	5235.66	5231.48	4200.39	4198.93	7310.82	7308.62	9352.36	9349.66
	6	5230.35	5227.12	4197.22	4194.33	7306.41	7303.49	9349.24	9347.25
	12	5227.31	5225.36	4193.63	4191.47	7301.17	7300.89	9345.39	9346.14

*Ref. [11]

Table 3
The natural frequencies ω_{ij} (Hz) of the plate with periodic radial through crack emanating from outer boundary for the different boundary conditions

Modes (i,j)	Number of cracks	F-C The length of cracks		C-F The length of cracks		C-C The length of cracks		S-S The length of cracks	
		40 mm	75 mm	40 mm	75 mm	40 mm	75 mm	40 mm	75 mm
(0,0)	4	482.18	480.95	230.22	228.11	1726.36	1724.21	833.73	831.21
	6	480.13	479.38	228.19 (249)*	226.71 (233)*	1723.47	1720.89	831.52	829.39
	12	477.96	476.66	227.13	225.54	1721.22	1718.91	830.13	828.11
(1,0)	4	883.91	881.26	204.85	203.17	1754.44	1752.58	927.11	925.37
	6	882.14	879.25	200.77 (180)*	201.83 (201)*	1752.32	1750.64	925.81	923.23
	12	879.64	877.42	201.33	200.06	1749.88	1747.97	924.41	921.99
(2,0)	4	1454.61	1452.23	313.77	312.28	2032.52	2029.16	1261.14	1258.71
	6	1452.43	1453.22	311.76	313.32	2031.31	2030.51	1258.73	1254.55
	12	1453.33	1448.48	310.58	310.16	2028.91	2027.42	1256.76	1255.27
(3,0)	4	2558.35	2555.52	561.56	555.74	2515.62	2511.61	1715.02	1712.62
	6	2556.95	2553.92	555.88 (491)*	556.14 (516)*	2513.78	2512.67	1713.08	1713.04
	12	2555.63	2550.14	551.89	550.33	2510.82	2508.75	1711.65	1709.88
(4,0)	4	7569.22	7566.72	1742.32	1738.97	4762.54	4758.57	4553.44	4550.41
	6	7567.14	7567.92	1740.23	1739.77	4759.74	4756.71	4554.06	4551.27
	12	7565.43	7563.24	1736.97	1735.12	4758.19	4753.43	4550.64	4548.72
(5,0)	4	3405.74	3403.42	2266.85	2259.84	6650.22	6645.45	5218.88	5215.62
	6	3407.29	3401.73	2263.16	2261.08	6647.43	6646.64	5214.93	5212.35
	12	3403.55	3400.02	2260.15	2255.06	6645.27	6642.87	5211.72	5209.81
(6,0)	4	6775.96	6773.95	2663.63	2657.12	9319.55	9314.45	5405.16	5399.53
	6	6777.44	6775.24	2660.65	2659.13	9316.77	9315.72	5407.38	5401.59
	12	6772.03	6771.17	2657.29	2653.38	9314.84	9311.69	5401.91	5395.51
(0,1)	4	2092.77	2090.01	1723.32	1722.03	5626.66	5623.44	3143.45	3141.24
	6	2090.22	2088.42	1720.34	1717.24	5623.16	5619.65	3140.35	3139.79
	12	2087.43	2083.94	1718.38	1714.63	5621.24	5617.52	3137.76	3136.14
(0,2)	4	4123.42	4121.75	7620.23	7618.59	12331.61	12327.12	7011.57	7009.29
	6	4118.19	4116.34	7617.53	7615.92	12323.94	12320.37	7008.92	7007.64
	12	4112.21	4111.02	7615.02	7614.07	12312.23	12308.16	7007.14	7004.13
(1,1)	4	2183.47	2180.44	1807.56	1803.66	5743.57	5740.08	3345.16	3342.62
	6	2180.83	2177.51	1805.22	1800.72	5740.44	5735.14	3341.44	3340.91
	12	2178.13	2175.42	1804.05	1798.91	5738.21	5733.67	3340.24	3339.21
(2,1)	4	2661.14	2658.37	2054.92	2049.33	7130.55	7127.51	3744.55	3735.66
	6	2659.33	2655.84	2051.32	2047.13	7126.25	7124.91	3741.77	3731.83
	12	2655.37	2654.13	2050.21	2044.11	7124.71	7122.41	3739.84	3728.04
(3,1)	4	4292.83	4290.23	2509.14	2502.81	7563.31	7560.52	4465.79	4462.87
	6	4290.10	4288.64	2507.46	2501.07	7561.66	7558.91	4463.11	4459.89
	12	4287.11	4284.88	2506.42	2498.78	7558.24	7555.45	4459.99	4457.18
(4,1)	4	3363.36	3358.12	3470.61	3466.31	8455.56	8452.62	7923.32	7921.91
	6	3356.21	3355.47	3468.32	3463.51	8451.81	8449.22	7921.46	7916.81
	12	3352.18	3350.98	3464.81	3459.84	8449.57	8446.26	7915.52	7913.74
(1,2)	4	5242.17	5240.62	4201.53	4200.02	7311.13	7310.75	9356.61	9353.71
	6	5237.44	5235.13	4198.39	4196.92	7310.24	7307.91	9349.24	9348.25
	12	5235.34	5232.37	4196.49	4193.17	7307.02	7305.72	9347.24	9348.88

*Ref. [11]

the same nodal diameters of the mode shapes and therefore at the most moving regions of this plate, the decline in the natural frequencies and the relative changes in the mode shapes are higher as seen in Fig. 6b.

In Figs. 7 and 8, how the mode shapes (2,0) and (3,0) change according to the radial cracks which are located at the most remote and the closest regions to the nodal diameters is presented as contour graphs. When Table 1 and Figs. 7 and 8 are scrutinized together, it is obvious that the radial cracks located at the 7, 19, 31 and 43 sector groups which are far from the nodal diameters in mode shape (2,0) and similarly at the 5, 13, 21, 29, 37, and 45 sector groups in mode shape (3,0) change the mode shapes to a higher extent and in these situations, natural frequencies decline more.

The natural frequencies of the plate change very small, when the locations of cracks are chosen close to the nodal points of each mode shape. The large drop in the natural frequencies is observed, if the locations of cracks are located at the farthest situation from nodal points of the plate.

The first 14 natural frequencies of the annular plate with periodic radial through cracks emanating from the inner and outer boundary are shown in Tables 2 and 3, respectively. The obtained results are compared to the experimental results in Ref. [11].

Tables 2 and 3 prove that rises in the cracks both in number and length on the annular plates with radial through cracks have reducing effects on the natural frequencies. Furthermore, it is obvious that the natural frequencies of some of the annular plates with cracks tend to increase in opposition to expectations of lower values, compared to the natural frequencies of the plates with less and shorter cracks. A comparison of the numerical values is presented in Tables 2 and 3 in the shaded area. These natural frequencies occur in the mode shapes where nodal circles are zero. It can be said that the difference stems from the lower depressing impact of the annular plates on the natural frequencies in the modes where radial through cracks are closer to nodal diameters. It is striking to obtain the same outcome when these results are compared to the experimental results of Ref. [11].

At the same time, the effects on the natural frequencies of annular plate with radial through cracks for four boundary conditions are shown in Tables 2 and 3. It is not possible to say directly about the effects of boundary conditions on the natural frequencies of the investigated plate.

5. Conclusions

The effect of cracks on the natural frequencies of annular plates has been analyzed theoretically via the finite element method. The sector type element with radial through crack of four nodes and three dof at each node is considered. If the sector angle of the annular plate is chosen properly, taking into account the nearness of the geometries of the sector and trapezoidal type element, the flexibility matrix of the sector type element with crack is derived by means of the flexibility matrix of the trapezoidal type element. The largest change in the natural frequencies is observed when the radial cracks are located at the farthest points from the nodal diameters of the plate. The smallest changes are occurred when the radial cracks are located at the nearest points to the nodal diameters of each diametral mode shape. The natural frequencies of some of the annular plates with cracks tend to increase in opposition to expectations of lower values, compared to the natural frequencies of the plates with less and shorter cracks. These natural frequencies occur in the mode shapes where nodal circles are zero. The same tendency is also observed with the existing experimental results of the literature. The theoretical results are obtained with different boundary conditions for the higher modes. It has been shown that the present sector type element can be used for the dynamic analysis of annular plates with radial cracks.

References

[1] A.D. Dimarogonas, Vibration of cracked structures: a state of the art review, *Engineering Fracture Mechanics* 55 (1996) 831–857.
[2] B. Stahl, L.M. Keer, Vibration and stability of cracked rectangular plates, *International Journal of Solids and Structures* 8 (1972) 69–91.
[3] R. Solecki, Bending vibration of a simply supported rectangular plate with a crack parallel to one edge, *Engineering Fracture Mechanics* 18 (1983) 1111–1118.
[4] G.L. Qian, S.N. Gu, J.S. Jiang, A finite element model of cracked plates and applications to vibration problems, *Computers and Structures* 39 (1991) 483–487.
[5] H.P. Lee, S.P. Lim, Vibration of cracked rectangular plates including transverse shear deformation and rotary inertia, *Computers and Structures* 49 (1993) 715–718.
[6] M. Krawczuk, Natural vibrations of rectangular plates with a through crack, *Archive of Applied Mechanics* 63 (1993) 491–504.
[7] K.M. Liew, K.C. Hung, M.K. Lim, A solution method for analysis of cracked plates under vibration, *Engineering Fracture Mechanics* 48 (1994) 393–404.
[8] S.E. Khadem, M. Rezaee, An analytical approach for obtaining the location and depth of an all-over part-through crack on externally in-plane loaded rectangular plate using vibration analysis, *Journal of Sound and Vibration* 230 (2000) 291–308.
[9] M. Krawczuk, A. Zak, W. Ostachowicz, Finite element model of plate with elasto-plastic through crack, *Computers and Structures* 79 (2001) 519–532.

[10] P. Lee, Fundamental frequencies of annular plates with internal cracks, *Computers and Structures* 43 (1992) 1085–1089.
[11] K. Ramesh, D.P.S. Chauhan, A.K. Mallik, Free vibration of an annular plate with periodic radial cracks, *Journal of Sound and Vibration* 206 (1997) 266–274.
[12] N.K. Anifantis, R.L. Actis, A.D. Dimarogonas, Vibration of cracked annular plates, *Engineering Fracture Mechanics* 49 (1994) 371–379.
[13] J. Yuan, P.G. Young, S.M. Dickinson, Natural frequencies of circular and annular plates with radial or circumferential cracks, *Computers and Structures* 53 (1994) 327–334.
[14] J.S. Przemieniecki, *Theory of Matrix Structural Analysis*, McGraw-Hill Company, New York, 1968.